Journal of Hazardous Materials 378 (2019) 120593

Contents lists available at ScienceDirect

Journal of Hazardous Materials

journal homepage: www.elsevier.com/locate/jhazmat

A new and practical Se(IV) removal method using Fe^{3+} type cation exchange resin

Daisuke Kawamoto[a,b,*], Yui Yamanishi[b], Hironori Ohashi[c], Kotaro Yonezu[d], Tetsuo Honma[e], Takeharu Sugiyama[f], Yasuhiro Kobayashi[g], Yoshihiro Okaue[b], Akane Miyazaki[a], Takushi Yokoyama[b,*]

[a] Department of Chemical and Biological Sciences, Faculty of Science, Japan Women's University, 2-8-1 Mejirodai, Bunkyo-ku, Tokyo, 112-8681, Japan
[b] Department of Chemistry, Faculty of Science, Kyushu University, 744 Motooka, Nishi-ku, Fukuoka, 819-0395, Japan
[c] Faculty of Symbiotic Systems Science, Fukushima University, 1 Kanayagawa, Fukushima, 960-1296, Japan
[d] Department of Earth Resources Engineering, Faculty of Engineering, Kyushu University, 744 Motooka, Nishi-ku, Fukuoka, 819-0395, Japan
[e] Japan Synchrotron Radiation Research Institute (JASRI), SPring-8, 1-1-1 Kouto, Sayo-cho, Sayo-gun, Hyogo, 679-5198, Japan
[f] Research Center for Synchrotron Light Applications, Kyushu University, 6-1 Kasuga-koen, Kasuga, Fukuoka, 816-8580, Japan
[g] Institute for Integrated Radiation and Nuclear Science, Kyoto University, 2 Asashiro-Nishi, Kumatori-cho, Sennan-gun, Osaka, 590-0494, Japan

ARTICLE INFO

Keywords:
Environmental preservation
Se pollution
Removal of selenium
Cation exchange resin adsorbing ferric ions

ABSTRACT

An effective method for removing selenium (Se) from water is required from the viewpoint of environmental preservation. To establish this method, a cation exchange resin that adsorbed ferric ions was applied as an adsorbent. In this study, the adsorption behavior of Se to the adsorbent was examined by both batch and column methods. The batch experiment confirmed that selenite ions (Se(IV)) are effectively adsorbed but selenate ions (Se(VI)) are hardly adsorbed. To elucidate the adsorption mechanism, the Fe in the adsorbent and the Fe in the adsorbent after the adsorption of Se(IV) were characterized by Fe K-edge X-ray absorption spectroscopy and ^{57}Fe Mössbauer spectroscopy. The analytical result of Se K-edge EXAFS spectra for the Se(IV) adsorbed on the adsorbent suggests that Se(IV) are adsorbed specifically to the adsorbent through the formation of Fe-O-Se bonds. The breakthrough curve obtained by the column experiment showed that Se(IV) in 3 tons of synthetic solution containing 0.1 ppm Se can be efficiently removed using a column in which 12.8 g (10.4 cm^3) of the adsorbent was packed.

1. Introduction

Selenium (Se) is a trace essential nutrient for living organisms. When it is lacking, organismal health is damaged. However, when living organisms are exposed to high concentrations of Se, they are poisoned. The optimum Se concentration range between deficiency and excess is quite narrow [1,2]. In particular, Se pollution is a serious problem in freshwater ecosystems. For example, there are some reports of teratogenic deformities [3] and decreased propagation abilities [4] in the fish stocks of America and Canada. In 1984, there was a case in which the groundwater was contaminated by Se due to the transport of wastewater from agricultural activities, namely, irrigating farmland and many birds died due to its biological concentration [5]. Therefore, it is important to monitor the Se concentration in natural waters. On the other hand, Se, which is a rare metal, is often used to produce ceramics and catalysts. In addition, it is also used in the medical and agricultural fields because it is an essential element for living organisms. Accordingly, the development of an efficient Se recovery method is required from the viewpoints of environmental preservation and industrial activity.

Se is present as selenite ion (SeO_3^{2-}, Se(IV)) and selenate ion (SeO_4^{2-}, Se(VI)) in oxidative environments depending on the pH and redox potential. To remove Se(IV), coprecipitation [6,7] and adsorption methods [8–11] have been reported, but no method has been published on the effective removal of Se(VI). At present, the coprecipitation and adsorption methods are used to remove Se from agricultural and industrial wastewater after reducing of Se(VI) to Se(IV) [12–15]. In the coprecipitation method, the generation of a large amount of sludge is the downside, which should be improved.

Iron (Fe) is widely distributed in soil, especially goethite (FeOOH),

* Corresponding authors at: Department of Chemical and Biological Sciences, Faculty of Science, Japan Women's University, 2-8-1 Mejirodai, Bunkyo-ku, Tokyo, 112-8681, Japan.
E-mail addresses: kawamotod@fc.jwu.ac.jp (D. Kawamoto), yokoyamatakushi@chem.kyushu-univ.jp (T. Yokoyama).

https://doi.org/10.1016/j.jhazmat.2019.04.076
Received 8 February 2019; Received in revised form 20 April 2019; Accepted 22 April 2019
Available online 31 May 2019
0304-3894/

which is an oxyhydroxide, and hematite (Fe_2O_3) and magnetite (Fe_3O_4), which are oxides, act as Se adsorbents [8,16,17]. According to a previous paper [18], they can adsorb both Se(IV) and Se(VI) equally well. Using iron compounds is an environment-friendly method. To avoid generating a large amount of sludge, the column method is preferable. To use the column method for removing harmful elements, developing the adsorbent is essential. When ferric ions are adsorbed onto cation exchange resin, the anion is also adsorbed, which is called "coadsorption" [19,20]. Therefore, in this study, the availability of a cation exchange resin adsorbing ferric ions (Fe^{3+} type CER) was examined for the removal of Se because of the easy desorption of ferric ions as $[FeCl_4]^-$ complex ion using a small amount of 6 mol/dm^3 hydrochloric acid and the quick regeneration to follow as described later. First, the Se (IV) adsorption behavior to the Fe^{3+} type CER was examined by batch method. Second, the Se(IV) removal ability of the Fe^{3+} type CER was evaluated by column method. Third, to elucidate the Se(IV) adsorption mechanism to the Fe^{3+} type CER, the ferric ions and Se(IV) adsorbed on the cation exchange resin were characterized by X-ray absorption (XA) spectroscopy and ^{57}Fe Mössbauer spectroscopy. Knowledge of the adsorption mechanism is important and basic information for enhancing the Se(IV) removal ability of Fe^{3+} type CER.

2. Experimental

2.1. Chemicals and sample solutions

The strong acid-type cation exchange resin used in this study was UBK 10 (Na type, Mitsubishi Chemical Co. Ltd.). The cation exchange capacity of the Na type UBK 10 was 2.2 meq/cm^3 and the degree of crosslinking was 10%. The cation exchange resin adsorbing ferric ions (called Fe^{3+} type UBK 10 here) was prepared by adding the Na type UBK 10 of 40 g into 0.1 mol/dm^3 $FeCl_3$ solution of 500 cm^3 and stirred with a shaker for 24 h. The resin was filtered by a 0.45 μm membrane filter and air-dried for 3 days. According to the Fe concentration determination of the filtrate by atomic absorption spectroscopy (AAS: AA-6300, Shimadzu, Japan), the amount of Fe adsorbed on the UBK 10 was estimated to be 0.84 mmol/g-dry resin. For Se(IV) and Se(VI), Na_2SeO_3 and Na_2SeO_4 were purchased from Wako Pure Chemicals. The reagents used in this investigation were of analytical grade. The sample solutions were prepared using deionized-distilled water. The stock solutions of Se (IV) and Se(VI) were prepared by dissolving the Na_2SeO_3 and Na_2SeO_4 in water.

FeOOH was used as a ferric oxyhydroxide standard for measuring of ^{57}Fe Mössbauer spectra and XA spectra, and was prepared according to the literature [21]. $Fe_2(SeO_3)_3$ was the ferric selenite standard and was prepared according to the literature [22].

2.2. Adsorption experiment by batch method

Se(IV) and Se(VI) solutions (2.5 ppm Se) with or without NaCl were prepared. The pH values of the solutions were adjusted using HNO_3. An adequate amount of the Fe^{3+} type UBK 10 was added to the Se(IV) and Se(VI) solutions (250 cm^3) and stirred with a shaker. At adequate intervals, aliquots of the suspended solution were collected and filtered with a 0.45 μm membrane filter. The Se concentration in the filtrates was determined by inductively coupled plasma atomic emission spectrometry (ICP-AES: Optima 5300 DV, PerkinElmer Inc.) to estimate the amount of Se adsorbed on the Fe^{3+} type UBK 10. The relative error of the Se determination by ICP-AES was within 5.59%. Moreover, whether ferric ion was desorbed or not was confirmed.

2.3. Adsorption experiment by column method

A breakthrough curve for Se(IV) was made using a glass column (1.5 cm diameter and 14 cm height). The Fe^{3+} type UBK 10 (12.8 g, 10.4 cm^3), which was swollen, was packed into the column. A 100 ppm Se(IV) solution was introduced into the column and a constant volume of effluent (320 cm^3) was collected in a plastic bottle as each fraction. Total volume of the effluent collected from the column was 5424 cm^3 to make a breakthrough curve for Se(IV). The flow rate was approximately 0.010 cm^3/sec. The NaCl concentration of the Se(IV) solution was 0.1 mol/dm^3 and the pH was 3. The Se concentration in the fraction was determined by ICP-AES.

2.4. Measurement of X-ray absorption (XA) spectra

The Fe K-edge and Se K-edge XA spectra were measured for the standard samples, the Fe^{3+} type UBK 10 and the Fe^{3+} type UBK 10 adsorbing Se(IV) (Se(IV)/Fe = 0.33 and 0.52) at SPring-8 BL14B2 (at 8 GeV and 99.5 mA). The Fe K-edge XA spectra were also measured for the standard samples and the Fe^{3+} type UBK 10 adsorbing Se(IV) (Se (IV)/Fe = 0.15) at SAGA-LS BL06 (at 1.4 GeV). In the measurement at the SPring-8, the Fe^{3+} type UBK 10 and the Fe^{3+} type UBK 10 adsorbing Se(IV) were ground using an agate mortar and the powder was diluted with boron nitride to make a pellet. Each sample was measured in transmission mode at ambient temperature. In the SAGA-LS, the Fe^{3+} type UBK 10 adsorbing Se(IV) was measured in fluorescence mode at ambient temperature. The spectra were analyzed using software (Athena of Ifeffit) [23].

2.5. Measurement of ^{57}Fe Mössbauer spectra

The ^{57}Fe Mössbauer spectra for FeOOH, $Fe_2(SeO_3)_3$ and ferric ions adsorbed on Chelex 100 (Fe^{3+} type Chelex 100) [24] were measured at Radioisotope (RI) center of Kyushu University. The ^{57}Fe Mössbauer spectra for Fe adsorbed on the Fe^{3+} type UBK 10 before and after the adsorption of Se(IV) were measured at the Research Reactor Institute of Kyoto University. The measurement was performed in transmission method. The γ-ray source was ^{57}Co/Rh (half-life: 271.74 d). The zero velocity position of the spectrum is the center of gravity for the α-Fe foil. The spectra were analyzed using computer software by assuming that each spectrum consists of a Lorentzian function.

3. Results and discussion

3.1. Adsorption experiment by batch method

3.1.1. Adsorption of Se(IV) and Se(VI)

Fig. 1 shows the variation in adsorption proportions for Se(IV) and Se(VI) to the Fe^{3+} type UBK 10 with time in the absence and presence of NaCl (0.1 mol/dm^3). The solution pH was 3, as described later. No Se (VI) was adsorbed, independent of the absence or presence of NaCl. On

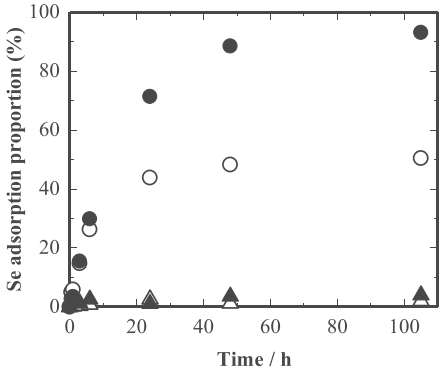

Fig. 1. Variation in the adsorption proportion of Se(IV) and Se(VI) with time in the absence (Se(IV): ○, Se(VI): △) and presence (0.1 mol/dm^3) of NaCl (Se(IV): ●, Se(VI): ▲). pH 3. Solution volume: 250 cm^3. Amount of Fe^{3+} type UBK 10 added: 0.2 g (0.17 mmol as Fe). Initial Se concentration: 2.5 ppm. Reaction time: 105 h.

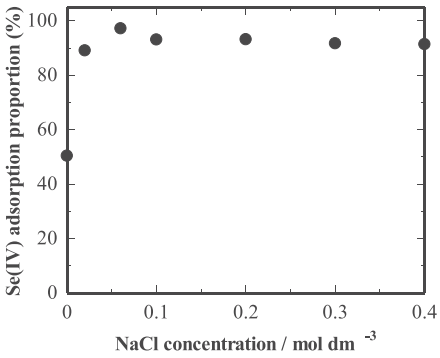

Fig. 2. Effect of the NaCl concentration on the adsorption proportion of Se(IV). pH 3. Solution volume: 250 cm^3. Amount of Fe^{3+} type UBK 10 added: 0.2 g (0.17 mmol as Fe). Initial Se concentration: 2.5 ppm. Reaction time: 48 h.

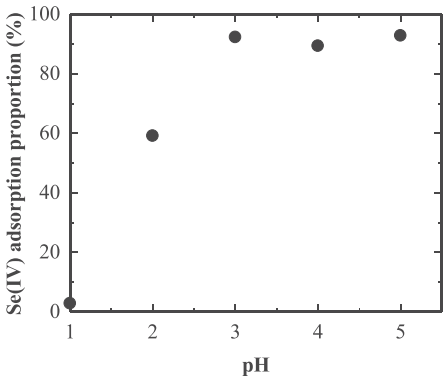

Fig. 3. Effect of the pH on the adsorption proportion of Se(IV). pH 3. NaCl concentration: 0.1 mol/dm^3. Solution volume: 250 cm^3. Amount of Fe^{3+} type UBK 10 added: 0.2 g (0.17 mmol as Fe). Initial Se concentration: 2.5 ppm. Reaction time: 48 h.

the other hand, the Se(IV) adsorbed onto the Fe^{3+} type UBK 10 with time. Interestingly, the adsorption proportion in the presence of NaCl was larger than that in the absence of NaCl. In the absence and presence of NaCl, the adsorption proportion of Se(IV) were 50.4% and 93.1%, respectively. Adsorption equilibrium may be attained after 48 h.

3.1.2. Effect of the NaCl concentration on the adsorption of Se(IV)

Since the adsorption of Se(IV) to the Fe^{3+} type UBK 10 was accelerated by the presence of NaCl, the effect of the NaCl concentration was examined. Fig. 2 shows the variation in the adsorption proportion of Se(IV) as the NaCl concentration ranged from 0 - 0.4 mol/dm^3. In the absence of NaCl, the adsorption proportion of Se(IV) is approximately 50%. On the other hand, the proportion of Se(IV) increased abruptly to approximately 90% when the NaCl concentration was 0.025 mol/dm^3. The adsorption proportion increased slightly, with increases above 0.025 mol/dm^3. The adsorption proportion was constant at more than 90% above 0.1 mol/dm^3 NaCl. In the electrostatic adsorption of cations and anions on the surface of metal oxides and hydroxides, the adsorption is generally retarded with the increased supporting electrolyte concentration [25,26]. Accordingly, Se(IV) may be adsorbed specifically on the Fe^{3+} type UBK 10.

Matsuura et al. reported that the ferric ion was adsorbed by a bidentate coordination on a cation exchange resin ($(-S)_2FeOH$, S: cation exchange site) above pH 2, and the ferric ion formed a single bond with Se(IV) ($(-S)_2FeOSeO_2H$) by coadsorption between the ferric ion and Se (IV) on a cation exchange resin [19]. This result suggests that Se(IV) formed a single bond with a ferric ion on the Fe^{3+} type UBK 10 in the absence of NaCl. On the other hands, Hayes et al., reported that the adsorption proportion of Se(IV) was increased by the formation of the ion pair of Na^+ and Se(IV) which was adsorbed on goethite in the presence of NaCl [26]. From these previous work, the cause for the increasing adsorption proportion of Se(IV) on the Fe^{3+} type UBK 10 in presence of NaCl was concluded to be the ion pair formation of Na^+ and Se(IV), and this pair was adsorbed on the Fe^{3+} type UBK 10.

3.1.3. Effect of the pH on the adsorption of Se(IV)

Because metal oxides and hydroxides have an isoelectric point, the adsorption of cations and anions is often affected by the pH [17]. Therefore, the effect of the pH on the adsorption of Se(IV) was examined over a pH range from 1 to 5. Fig. 3 shows the variations in the Se(IV) adsorption proportion with the pH. With the increasing pH, the adsorption proportion increased and reached a constant value of more than 90% above pH 3. According the previous studies [8,11], the adsorption proportion of Se(IV) onto iron(III) (hydr)oxide is the almost same at pH 4-8. Since it was considered that the Se(IV) removal ability of the Fe^{3+} type UBK 10 is the almost same even above pH 3, the adsorption behavior of Se(IV) was examined at pH 3 that is the lower limit of pH value for the efficient removal of Se(IV) from 2.5 ppm Se solution.

According to the previous study [27], in the presence of PO_4^{3-}, the adsorption proportion of Se(IV) to goethite decreases with the increasing pH. When the Fe^{3+} type UBK 10 is applied the removal of Se (IV) from a real polluted water including PO_4^{3-} as a competitive ion, the adsorption of Se(IV) proceeds effectively, while, the interference by PO_4^{3-} to the Se(IV) adsorption becomes also stronger. Consequently, pH 3 was selected as an optimum pH for the adsorption experiment because it maintained a balance between the efficient adsorption of Se(IV) (higher pH) and the retardation of interference by anion to the adsorption (lower pH).

3.1.4. Adsorption isotherm for Se(IV)

To make an adsorption isotherm, adsorption experiments were performed under various concentrations of Se(IV) (0–11 mmol/dm^3). The adsorption isotherm is shown in Fig. 4a. The Se/Fe atomic ratio, which corresponds to the amount of Se(IV) adsorbed on the Fe^{3+} type UBK 10, ranged from 0.04 to 0.69. The experimental conditions are described in the figure caption. The adsorption isotherm obtained here fit well to the Langmuir type as expressed by Eq. (1).

$$N = {N^{\infty}KC}/{(1 + KC)} \quad (1)$$

Here, N indicates the amount of Se(IV) adsorbed on the Fe^{3+} type UBK 10 (mmol/g), N^{∞} is the saturation amount of Se(IV) (mmol/g), K is the equilibrium constant for adsorption ((mmol/dm^3)$^{-1}$), and C is the equilibrium concentration of Se(IV) in solution (mmol/dm^3). If the isotherm fits the Langmuir type, when the C/N is plotted against C, a straight line with a slope of $1/N^{\infty}$ and an intercept of $1/(N^{\infty}K)$ should be obtained. The analytical result is shown in Fig. 4b. The correlation coefficient (R^2) was 0.999(7). The parameters, N^{∞} and K, were estimated to be 0.58 and 16.6, respectively.

3.1.5. Interference of anions

When considering agricultural wastewater, Cl^-, HCO_3-, NO_3^-, SO_4^{2-} and PO_4^{3-} ions are candidate interfering ions in the adsorption of Se(IV) onto the Fe^{3+} type UBK 10. Cl^- and NO_3^- scarcely adsorb onto the surface of ferric hydroxide but HCO_3-, SO_4^{2-} and PO_4^{3-} can be significantly adsorbed [28]. Therefore, it is considered that no Cl^- and NO_3^- adsorbed onto the Fe^{3+} type UBK 10. No HCO_3- exists at the pH investigated this study (pH3–5) because H_2CO_3 (pK_1 = 6.11 and pK_2 = 9.87) is the predominant species. Therefore, the influence of HCO_3^- is not necessary to be considered. Fig. 5 shows the interference of SO_4^{2-} and PO_4^{3-} on the adsorption of Se(IV) to the Fe^{3+} type UBK 10. The adsorption proportion of Se(IV) decreased with the increasing SO_4^{2-} and PO_4^{3-} concentrations and the Se(IV) hardly adsorbed at 1000 ppm of both ions. SO_4^{2-} and PO_4^{3-} interfered with the adsorption of Se(IV) above 100 ppm and 10 ppm, respectively. Practically, it is necessary to consider the interference of PO_4^{3-}.

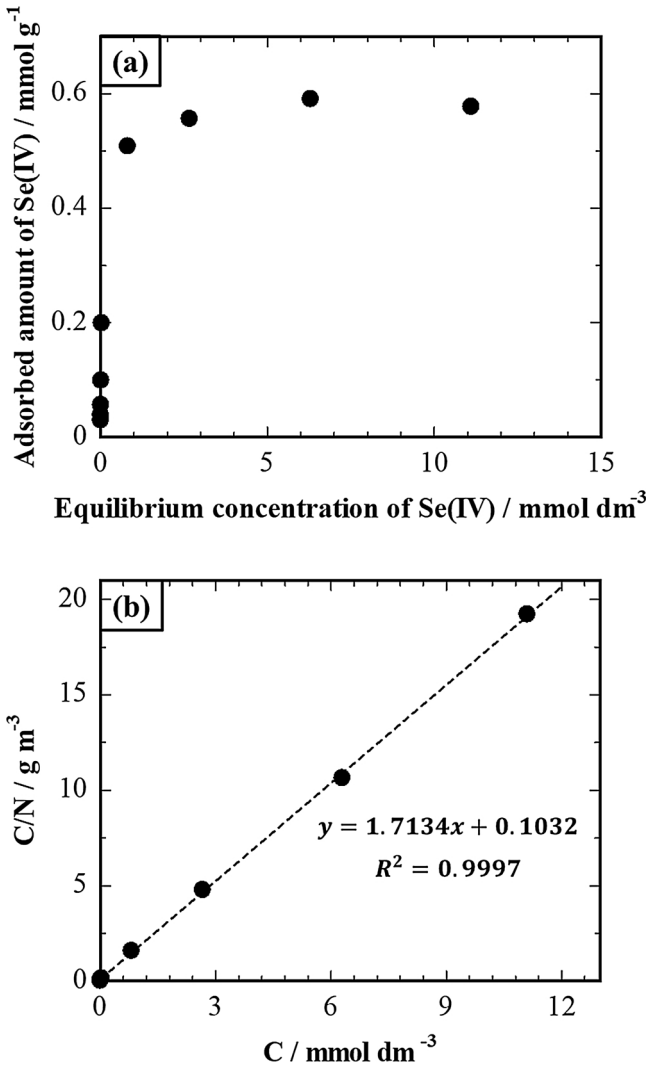

Fig. 4. Adsorption isotherm for Se(IV) (a) and the analytical result (b). pH 3. NaCl concentration: 0.1 mol/dm^3. Amount of Fe^{3+} type UBK 10 added: 0.2 g (0.17 mmol as Fe). Reaction time: 48 h.

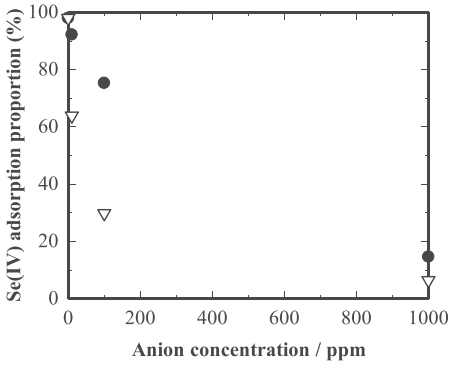

Fig. 5. Effect of SO_4^{2-} (●) and PO_4^{3-} (▽) ion concentrations on Se(IV) adsorption. pH 3. NaCl concentration: 0.1 mol/dm^3. Solution volume: 250 cm^3. Amount of Fe^{3+} type UBK 10 added: 0.2 g (0.17 mmol as Fe). Reaction time: 48 h.

3.2. Adsorption experiment by column method

To obtain the breakthrough curve, a Se(IV) solution was continuously introduced into a column packed with the Fe^{3+} type UBK 10. To shorten the experiment time, a 100 ppm Se (IV) solution was used.

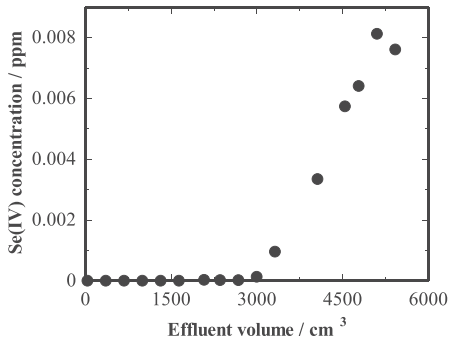

Fig. 6. A breakthrough curve for Se(IV). pH 3. Se (IV) concentration: 100 ppm. Size of column: diameter 1.5 cm and height 14 cm. Amount of Fe^{3+} type UBK 10 packed into the column: 10.4 cm^3 (12.8 g-dry, 0.84 mmol as Fe).

Fig. 6 shows a breakthrough curve for Se(IV). The horizontal axis indicates the effluent volume of solution from when the Se (IV) solution was introduced into the top of the column. The elution of Se(IV) from the column was begun at approximate 3000 cm^3 of the effluent volume. The emission standard limit for Se is 0.01 ppm according to the environmental laws of Japan. Based on the breakthrough curve in Fig. 6, if the Se concentration of a synthetic solution is 0.1 ppm, Se(IV) in 3 tons of the solution can be removed by a column packed with 12.8 g of the Fe^{3+} type UBK 10. To maintain equilibrium, the flow rate of solution through the column was approximately 0.010 cm^3/sec. Therefore, it will be necessary to examine the influence of the flow rate on removal ability before practical use.

3.3. Characterization for Fe and Se adsorbed on the Fe^{3+} type UBK 10

To maintain an adequate Se(IV) constant adsorption efficiency, it is important to investigate the adsorption mechanism of Se(IV) to the Fe^{3+} type UBK 10. To elucidate the adsorption mechanism, the existing states of the Fe and Se on the Fe^{3+} type UBK 10 were examined by XA spectroscopy (Fe and Se K-edge) and ^{57}Fe Mössbauer spectroscopy.

3.3.1. Fe K-edge XA spectra

Fig. 7 shows the Fe K-edge X-ray absorption near edge structure (XANES) spectra for FeOOH as a standard of ferric oxyhydroxide (a), the Fe^{3+} type UBK 10 (c) and the Fe^{3+} type UBK 10 adsorbing Se(IV)

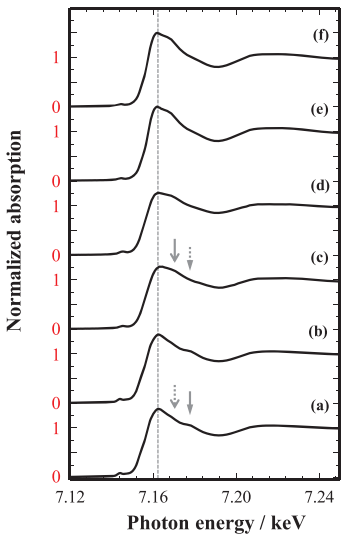

Fig. 7. Normalized Fe K-edge XANES spectra for FeOOH (a), FeOOH adsorbing Se(IV) (Se/Fe = 0.01) (b), Fe^{3+} type UBK 10 (c) and Fe^{3+} type UBK 10 adsorbing Se(IV) (Se/Fe = 0.15, 0.33 and 0.52) (d)-(f). ↓ and ⇣: the presence and absence of a shoulder on the spectrum.

(Se/Fe = 0.15, 0.33 and 0.52) (d)-(f). In addition, to examine the change in the chemical state of Fe when Se(IV) is adsorbed onto the FeOOH, the FeOOH adsorbing Se(IV) (b) was also measured.

All the spectra are considerably resemble, indicating that the valence state of Fe is trivalent. However, there are slight differences among the spectra. All the spectra show the peak top to be approximately 7.16 keV, but the energy is slightly different, that is, the energy of the peak for FeOOH (a) is lower than that of the Fe^{3+} type UBK 10 (c). The spectrum for the Fe^{3+} type UBK 10 has a shoulder at approximately 7.17 keV (arrow of solid line), but there is no shoulder on the spectrum for FeOOH (arrow of dotted line). Moreover, the spectrum for FeOOH shows a small and broad peak at approcimately 7.18 keV (arrow of solid line), on the other hand, there is no peak at approximately 7.18 keV on the spectrum for the Fe^{3+} type UBK 10 (arrow of dotted line). These results suggest that the chemical state of Fe in the Fe^{3+} type UBK 10 is different from that of FeOOH. For the main absorption peak described above, although the energy of the peak top for FeOOH is almost the same as that of FeOOH adsorbing Se(IV), the energy of the peak top for the Fe^{3+} type UBK 10 adsorbing Se(IV) (d)-(f) shifted to the lower energy side compared to that for the Fe^{3+} type UBK 10. This result suggests that the electronic state of the Fe may be changed due to the adsorption of Se(IV) to the Fe^{3+} type UBK 10. In particular, it may be due to the formation of an Fe-O-Se bond. In addition to the main absorption peak, all the spectra show a small pre-edge peak at approximately 7.14 keV. Although the energy of the pre-edge peak for FeOOH is the same as that of FeOOH adsorbing Se(IV), the energy was different among Fe^{3+} type UBK 10 and Fe^{3+} type UBK 10 adsorbing Se(IV) depending on the amount of Se(IV) adsorbed. Fig. 8 shows an enlarged view of the pre-edge of the Fe K-edge XANES spectra for Fe^{3+} type UBK 10 (a) and Fe^{3+} type UBK 10 adsorbing Se(IV) (Se/Fe = 0.15, 0.33 and 0.52) (d)-(f). The result shows that the pre-edge peak shifted to the lower energy side with the increasing Se/Fe atomic ratio. This result also suggests that the electronic state of Fe may be changed due to the adsorption of Se(IV) to the Fe^{3+} type UBK 10 as indicated above.

3.3.2. *^{57}Fe Mössbauer spectra*

Fig. 9 shows the ^{57}Fe Mössbauer spectra for FeOOH (a), $Fe_2(SeO_3)_3$ (b), Fe^{3+} type Chelex 100 (functional group: iminodiacetate that is a tridentate ligand) (c) [24], the Fe^{3+} type UBK 10 (d) and the Fe^{3+} type UBK 10 adsorbing Se(IV) (Se/Fe = 0.52) (e). The ^{57}Fe Mössbauer parameters obtained here are also represented in Table 1. The iminodiacetate group is a functional group of chelate resin (Chelex 100), and because it is a tridentate ligand, each ferric ion is coordinated as an isolated ion. However, the sulfonate groups as functional groups of the cation exchange resin (UBK 10) attract cations such as ferric ions by

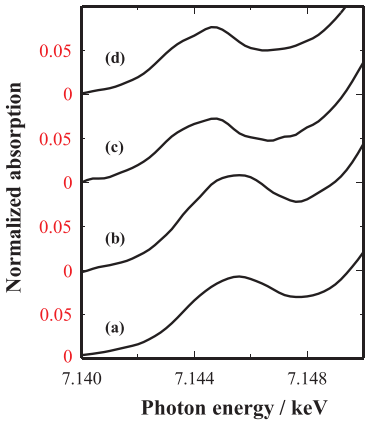

Fig. 8. Enlarged view of the pre-edge of the Fe K-edge XANES spectra for Fe^{3+} type UBK 10 (a) and Fe^{3+} type UBK 10 adsorbing Se(IV) (Se/Fe = 0.15, 0.33 and 0.52) (b)-(d).

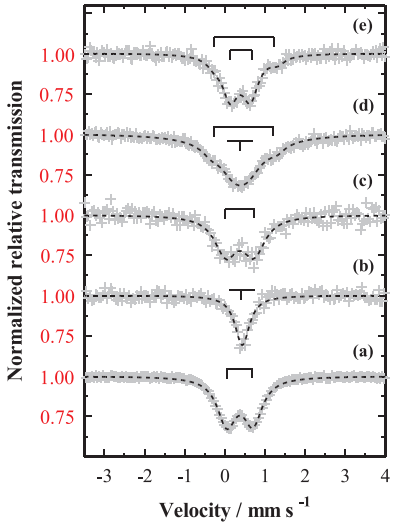

Fig. 9. ^{57}Fe Mössbauer spectra for FeOOH (a), $Fe_2(SeO_3)_3$ (b), Fe^{3+} type Chelex 100 (a standard for isolated ferric ion) (c), Fe^{3+} type UBK 10 (d) and Fe^{3+} type UBK 10 adsorbing Se(IV) (Se/Fe = 0.52) (e).

Table 1
^{57}Fe Mössbauer parameters.

	Component	IS [a] / mm s^{-1}	QS [b] / mm s^{-1}	FWHM [c] / mms^{-1}	Ratio of peak area
FeOOH	-	0.375	0.653	0.570	-
$Fe_2(SeO_3)_3$	-	0.435	-	0.434	-
Fe^{3+} type Chelex 100	-	0.377	0.700	0.654	-
Fe^{3+} type UBK 10	# 1	0.392	-	1.24	0.887
	# 2	0.477	1.65	0.475	0.113
Fe^{3+} type UBK 10 adsorbing Se(IV) (Se/Fe = 0.52)	# 1	0.386	0.499	0.487	0.876
	# 2	0.528	1.58	0.420	0.124

[a] Isomer shift.
[b] Quadrupole splitting.
[c] Full width at half maximum.

electrostatic interaction. As shown in Fig. 9 and Table 1, the spectrum for the Fe^{3+} type UBK 10 and its parameters are different from those of the Fe^{3+} type Chelex 100. From the analysis of the spectrum for Fe^{3+} type UBK 10, there are two different chemical states of ferric ions in the Fe^{3+} type UBK 10. The full width at half maximum (*FWHM*) value for the singlet (component #1) is larger than that for other samples, suggesting that the ferric ions adsorbed on UBK 10 may be present as hydrolytic cluster cations with Fe-O-Fe bonds consisting of different numbers of ferric ions according to the existing state of the ferric ions adsorbed on the cation exchange resin, as described by Matsuura [19]. The spectrum for component #1 and its parameters are different from those for FeOOH, which is an inorganic polymer with a long-range structure. In addition, the doublet (component #2) with a large quadrupole splitting (*QS*) value was observed, suggesting that the ferric ion is more distorted than that in other samples. The oxo-bridged ferric ion adsorbed on cation exchange resin ($[(\text{-S})_2(\text{Fe-O-Fe})(\text{S-})_2]$) has been reported as a species with a large *QS* value (1.66 mm/s) [19], where (-S) indicates sulfonate groups as a functional group. Therefore, the doublet of the spectrum for the Fe^{3+} type UBK 10 is assigned as the oxo-bridged ferric ion adsorbed on UBK 10.

Interestingly, the singlet for the Fe^{3+} type UBK 10 significantly changed when Se(IV) was adsorbed. However, the spectrum is different from that for $Fe_2(SeO_3)_3$. This result indicates that Se(IV) does not precipitate as $Fe_2(SeO_3)_3$ but adsorbs to the Fe^{3+} type UBK 10. On the other hand, the parameters for the doublet hardly changed before and

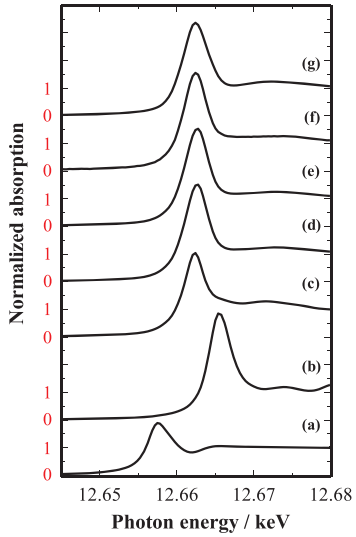

Fig. 10. Normalized Se K-edge XANES spectra for Se powder (a), Na_2SeO_4 (b), Na_2SeO_3 (c), and Fe^{3+} type UBK 10 adsorbing Se(IV) (Se/Fe = 0.33 and 0.52) (d) and (e), FeOOH adsorbing Se(IV) (Se/Fe = 0.01) (f) and $Fe_2(SeO_3)_3$ (g).

after Se(IV) adsorption.

3.3.3. Se K-edge XA spectra

To elucidate the bonding mode of Se adsorbed to the Fe^{3+} type UBK 10, the Se K-edge XA spectra were measured. Fig. 10 shows the Se K-edge XANES spectra for Se powder as a standard of Se(0) (a), Na_2SeO_4 as a standard of Se(VI) (b), Na_2SeO_3 as a standard of Se(IV) (c), the Fe^{3+} type UBK 10 adsorbing Se(IV) (Se/Fe = 0.33 and 0.52) (d) and (e), FeOOH adsorbing Se(IV) (Se/Fe = 0.01) (f) and $Fe_2(SeO_3)_3$ (g). From comparisons with the XANES spectra for standards of Se(0), Se (IV) and Se(VI), the Se adsorbed to the Fe^{3+} type UBK 10 is present as Se(IV). Moreover, the XANES spectrum for the Se(IV) adsorbed to the Fe^{3+} type UBK 10 is different from that of the $Fe_2(SeO_3)_3$. The energy of the peak top of the XANES spectrum for the Se(IV) adsorbed on the FeOOH is the same as that for Na_2SeO_3, while, the energy of the peak top for Se(IV) adsorbed to the Fe^{3+} type UBK 10 is slightly higher than that for Se(IV) adsorbed on FeOOH. This result suggests that the chemical state of Se(IV) adsorbed to the Fe^{3+} type UBK 10 is different from that on the FeOOH, although the difference is slight.

Fig. 11 shows the Fourier transform of the extended X-ray absorption fine structure (EXAFS) oscillation extracted from the Se K-edge XA spectra for the Fe^{3+} type UBK 10 adsorbing Se(IV) (Se/Fe = 0.33 and 0.52) (a) and (b), the FeOOH adsorbing Se(IV) (Se/Fe = 0.01) (c) and $Fe_2(SeO_3)_3$ (d). In Fig. 11, the first peaks at approximately 1.2 Å are due to Se-O interaction and the second peaks at approximately 2.7 Å are due to Se-Fe interaction. The appearance of the second peaks indicates that Se(IV) is specifically adsorbed to the Fe^{3+} type UBK 10 through the formation of an Fe-O-Se bond. The Se-O and Se-Fe distances are almost the same between Fe^{3+} type UBK 10 adsorbing Se(IV) and FeOOH adsorbing Se(IV), suggesting that the adsorption mode of Se(IV) is basically the same between the Fe^{3+} type UBK 10 and the FeOOH. In their EXAFS study, Hayes et al. (1987) reported that Se(IV) is adsorbed onto the surface of FeOOH as an inner sphere complex [29]. Peak and Sparks (2002) also reported that Se(VI) is adsorbed as inner and outer sphere complexes onto the surface of FeOOH depending on the ionic strength [30]. These results suggest that the Se(IV) is adsorbed onto the ferric ion in the Fe^{3+} type UBK 10 as an inner sphere complex. On the other hand, from the results of ^{57}Fe Mössbauer spectra and parameter, it is clear that no $Fe_2(SeO_3)_3$ is formed on the Fe^{3+} type UBK 10.

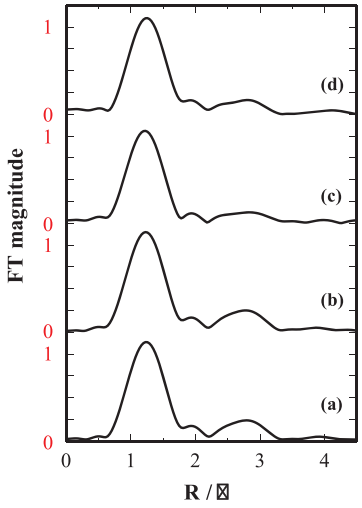

Fig. 11. Fourier transform of EXAFS oscillation extracted from Se K-edge XA spectra for Fe^{3+} type UBK 10 adsorbing Se(IV) (Se/Fe = 0.33 and 0.52) (a) and (b), FeOOH adsorbing Se(IV) (Se/Fe = 0.01) (c) and $Fe_2(SeO_3)_3$ (d). Fourier transform range: k = . 2.0–9.0.

3.4. Adsorption mechanism of Se(IV) to Fe^{3+} type UBK 10 and the desorption mechanism for regeneration of the column

From the characterization for the Fe^{3+} type UBK 10 by the Fe K-edge XA spectra and the ^{57}Fe Mössbauer spectra, it was suggested that the ferric ions that adsorbed on UBK 10 were present as hydrolytic cluster cations with Fe-O-Fe bonds consisting of different numbers of ferric ions.

The adsorption proportion of Se(IV) on the Fe^{3+} type UBK 10 increases with the increasing pH, as shown in Fig. 3. From a distribution curve for the Se(IV) against the pH derived from the dissociation constants of H_2SeO_3 (pK_1 = 2.61, pK_2 = 8.05), the adsorption proportion of Se(IV) increases with the increasing proportion of $HSeO_3^-$. Suggesting that $HSeO_3^-$ is adsorbed specifically on the Fe^{3+} type UBK 10. The adsorption of Se(IV) to the Fe^{3+} type UBK 10 was accelerated by the presence of NaCl. It is notable that $HSeO_3^-$ can form an ion pair (Na^+ $^-OSeO_2H$) with Na^+ in the presence of NaCl. Staicu et al. reported the selenium removal ability of a commercial iron oxide impregnated anion exchange resin from a synthetic solution and a real polluted water [31]. In the study, authors indicated that both of Se(IV) and Se(VI) were adsorbed onto the anion exchange site (quaternary ammonium group) of the iron oxide impregnated anion exchange resin, and the adsorption proportions of them from synthetic solution containing 5.0 ppm Se were the above 90% using the resin (1.7 g/L). On the other hand, based on the change in ^{57}Fe Mössbauer parameters before and after adsorption of Se(IV) to the Fe^{3+} type UBK 10, the $HSeO_3^-$ ion may be adsorbed to Fe^{3+} of the component #1 shown in Fig. 9 (a) and (e). While the adsorption proportions of Se(IV) from synthetic solution containing 2.5 ppm Se were approximately 100% using the resin (0.8 g/L), Se(VI) were adsorbed hardly onto the resin. Although it is necessary to pretreat using appropriate reducing reagents in order to reduce Se (VI) to Se(IV) in a real polluted water, the Fe^{3+} type UBK 10, which the chemical state of iron is different, is expected to demonstrate the same removal ability of Se(VI) as a commercial iron oxide impregnated anion exchange resin.

According to the previous study on the adsorption proportion of Fe^{3+} onto a cation exchange resin with the presence of HCl [32], the distribution coefficient of Fe^{3+} to the resin decreases with the increasing of the concentration of HCl. In addition, when the HCl concentration is 3.0 mol/dm^3, no Fe^{3+} is adsorbed onto cation exchange resin due to the formation of ferric-chloride complex ion (i.e. $[FeCl_4]^-$) [33]. Therefore, it was considered that Fe^{3+} and H_2SeO_3 are quickly

and easily desorbed from the Fe^{3+} type UBK 10 using a small amount of 6.0 mol/dm^3 HCl.

4. Conclusions

To develop an effective Se removal method using a column, the Fe^{3+} type UBK 10 was prepared and Se adsorption experiments were performed. The optimum conditions for Se adsorption onto Fe^{3+} type UBK 10 were established as follows: pH 3 and NaCl concentration = 0.1 mol/dm^3. In this investigation, the adsorption behavior of Se(IV) on the Fe^{3+} type UBK 10 was studied.

At pH 3, Se(IV) was adsorbed, while no Se(VI) was adsorbed. Surprisingly, the amount of Se(IV) adsorbed onto the Fe^{3+} type UBK 10 increased with the increasing ionic strength. This result is the opposite phenomenon in cases of Se adsorption onto the surface of ferric oxides and hydroxides. The adsorption isotherm of Se(IV) fit well to the Langmuir type. The saturation amount of adsorbed Se(IV) was an Se/Fe atomic ratio of 0.69.

From the ^{57}Fe Mössbauer spectra for the Fe^{3+} type UBK 10 and Fe^{3+} type UBK 10 adsorbing Se(IV), it was clear that the chemical state of Fe on the UBK 10 may be different from that of FeOOH and the chemical state was changed by the adsorption of Se(IV). The Se K-edge EXAFS spectra showed an interaction of Se-Fe in addition to an Se-O interaction, indicating that Se(IV) is specifically adsorbed onto the Fe^{3+} type UBK 10 by the formation of an Fe-O-Se bond.

When the Se(IV) solution containing 100 ppm Se was introduced into a column in which the Fe^{3+} type UBK 10 of 10. 39 cm^3 was packed, the Se concentration in the effluent from the column was lower than 0.01 ppm until the effluent volume reached 3000 cm^3.

From the high adsorption efficiency of Se(IV) and the high selectivity for adsorption of Se(IV) due to the formation of a Fe—O—Se bond, the Fe^{3+} type UBK 10 is a practical tool for removing Se(IV) from polluted water such as agricultural wastewater. However, the interference of PO_4^{3-} should be considered.

Acknowledgements

The cation exchange resin (UBK 10) used in this study was provided from MITSUBISHI CHEMICAL. The XA spectra measurement was conducted at BL14B2 in SPring-8 as a selected joint work (Project number: 2013A1820, 2014A1534, 2016B1560) and at BL06 in SAGA-LS as a selected joint work (Project number: 2013IIIK014).

References

[1] M. Alber, C. Demesmay, J.L. Rocca, Analysis of organic and nonorganic arsenious or selenious compounds by capillary electrophoresis, Fresenius J. Anal. Chem. 351 (1995) 426–432.
[2] P.M. Chapman, Invited debate/commentary: selenium – a potential time bomb or just another contaminant? Hum. Ecol. Risk Assess. 5 (1999) 1123–1138.
[3] J.M. Conley, D.H. Funk, D.B. Buchwalter, Selenium bioaccumulation and maternal transfer in the mayfly centroptilum triangulifer in a life-cycle, periphyton-biofilm trophic assay, Environ. Sci. Technol. 43 (2009) 7952–7957.
[4] D.K. DeForest, G. Gilron, S.A. Armstrong, E.L. Robertson, Species sensitivity distribution evaluation for selenium in fish eggs: considerations for development of a Canadian tissue-based guideline, integrated environ, Integrated Environ. Assess. Manag. 8 (2011) 6–12.
[5] L. Wu, Review of 15 years of research on ecotoxicology and remediation of land contaminated by agricultural drainage sediment rich in selenium, Ecotoxicol. Environ. Saf. 57 (2004) 257–269.
[6] J.M. Montgomery, Water Treatment Principle & Design, Consulting Engineers Inc., John Wiley & Sons, New York, 1985.
[7] D.T. Merrill, M.A. Manzione, J.J. Peterson, D.S. Parker, W. Chow, A.O. Hobbs, Field evaluation of arsenic and selenium removal by iron coprecipitation, J. Water Pollut. Control Fed. 58 (1986) 18–26.
[8] L.S. Balistrieri, T.T. Chao, Adsorption of selenium by amorphous iron oxyhydroxide and manganese dioxide, Geochim. Cosmochim. Acta 54 (1990) 739–751.
[9] S. Glasauer, H.E. Doner, A.U. Gehring, Adsorption of selenite to goethite in a flow through reaction chamber, Eur. J. Soil. Sci. 46 (1995) 47–52.
[10] E.I. EI-Shafey, Sorption of Cd(II) and Se(IV) from aqueous solution using modified rice husk, J. Hazard. Mater. 147 (2007) 546–555.
[11] N. Zhang, L.S. Lin, D. Gang, Adsorption selenite removal from water using iron-coated GAC adsorbents, Water Res. 42 (2008) 3809–3816.
[12] Y. Kashiwagi, E. Kokufuta, Selective determination of selenite and selenate in wastewater by graphite furnace AAS after iron(III) hydroxide coprecipitation and reductive coprecipitation on palladium collector using hydrazinium sulfate, Anal. Sci. 16 (2000) 1215–1219.
[13] M. Fujita, M. Ike, M. Kashiwa, R. Hashimoto, S. Soda, Laboratory-Scale Continuous Reactor for Soluble Selenium removal Using Selenate-Reducing Bacterium,*Bacillus* sp. SF1, Biotechnol. Bioeng. 80 (2002) 755–761.
[14] M. Lenz, E.D.V. Hullebusch, G. Hommes, P.F.X. Corvini, P.N.L. Lens, Selenate removal in methanogenic and sulfate-reducing upflow anaerobic sludge bed reactors, Water Res. 42 (2008) 2184–2194.
[15] T. Shoji, H. Uemoto, M. Morita, Development of Biological Selenate-reducing System for Flue-gas Desulfurization Wastewater Treatment – Optimization of Operational Conditions for Actual FGD Wastewater Treatment –, CRIEPI Research Report, (2012), p. V11059.
[16] M.O.M. Sharrad, H. Liu, M. Fan, Evaluation of FeOOH performance on selenium reduction, Sep. Purif. Technol. 84 (2012) 29–34.
[17] G. Zelmanov, R. Semiat, Selenium removal from water and its recovery using iron (Fe^{3+}) oxide/hydroxide-based nanoparticles sol (NanoFe) as an adsorbent, Sep. Purif. Technol. 103 (2013) 167–172.
[18] K. Fukushi, D.A. Sverjensky, A surface complexation model for sulfate and selenate on iron oxides consistent with spectroscopic and theoretical molecular evidence, Geochim. Cosmochim. Acta 71 (2007) 1–24.
[19] T. Matsuura, K. Ohnaka, M. Takagi, M. Ohashi, K. Mibu, A. Yuchi, Coadsorption of trivalent metal ions and anions on strongly acidic cation-exchange resins by bridge bonding, Anal. Chem. 80 (2008) 9666–9671.
[20] A. Yuchi, Diverse secondary interactions between ions exchanged into the resin phase and their analytical applications, Anal. Sci. 30 (2014) 51–57.
[21] U. Schwertmann, R.M. Cornell, Iron Oxides in the Laboratory: Preparation and Characterization Second Completely Revised and Extended Edition, WILEY-VCH, 2019.
[22] G. Giester, F. Pertlik, Synthesis and crystal structure of iron(III) selenate(IV) trihydrate, $Fe_2(SeO_3)_3{\cdot}3H_2O$, J. Alloys Compd. 210 (1994) 125–128.
[23] B. Ravela, M. Newville, ATHENA, ARTEMIS, HEPHAESTUS: data analysis for X-ray absorption spectroscopy using IFEFFIT, J. Synchrotron Rad. 12 (2005) 537–541.
[24] S. Aacharya, N. Gaowa, H. Ohashi, D. Kawamoto, T. Honma, Y. Okaue, T. Yokoyama, Adsorption behavior of arsenic to an isolated Ferric Ion combined on chelate resin, Bull. Chem. Soc. Jpn. 90 (2017) 1372–1374.
[25] K.F. Hayes, J.O. Leckie, Modeling ionic strength effects on cation adsorption at hydrous oxide/solution interfaces, J. Colloid Interface Sci. 115 (1987) 564–572.
[26] K.F. Hayes, C. Papelis, J.O. Leckie, Modeling ionic strength effects on anion adsorption at hydrous oxide/solution interfaces, J. Colloid Interface Sci. 125 (1988) 717–726.
[27] S. Goldberg, Chemical modeling of anion competition on goethite using the constant capacitance model, Soil Sci. Soc. Am. J. 49 (1985) 851–856.
[28] Y. Jiang, T. Yanagita, Tomoyo Mitani, Effects of coexisting anions on arsenite adsorption of newly developed iron hydroxide, J. Jpn. Soc. Water Environ. 37 (2014) 169–176.
[29] K.F. Hayes, A.L. Roe, G.E. Brown, K.O. Hodgson, J.O. Leckie, G.A. Parks, In situ x-ray absorption study of surface complexes: selenium oxyanions on α-FeOOH, Science 238 (1987) 783–786.
[30] D. Peak, D.L. Sparks, Mechanisms of selenate adsorption on iron oxides and hydroxides, Environ. Sci. Technol. 36 (2002) 1460–1466.
[31] L.C. Staicu, N. Morin-Crine, G. Crini, Desulfurization: critical step towards enhanced selenium removal from industrial effluents, Chemosphere 172 (2017) 111–119.
[32] J. Korkisch, S.S. Ahluwalia, Cation-exchange behavior of several elements in hydrochloric acid-organic solvent media, Talanta 14 (1967) 155–170.
[33] A.A.S. Aboul-Magd, S.A. Al-Husain, S.A. Al-Zahrani, Batch adsorptive removal of Fe (III), Cu(II) and Zn(II) ions in aqueous and aqueous organic-HCl media by Dowex $HYRW_2$-Na Polisher resin as adsorbents, Arab. J. Chem. 9 (2016) S1–S8.